Using Multiscale Ethane/Methane Observations to Attribute Coal Mine Vent Emissions in the San Juan Basin from 2013–2021

Aaron G. Meyer[1], Rodica Lindenmaier[1], Sajjan Heerah[1], Katherine B. Benedict[1], Eric A. Kort[2], Jeff Peischl[3,4], Manvendra K. Dubey[1]

[1] Earth and Environmental Sciences, Los Alamos National Laboratory, Los Alamos, NM, USA
[2] Climate and Space Sciences and Engineering, University of Michigan, Ann Arbor, MI, USA
[3] Cooperative Institute for Research in Environmental Sciences, University of Colorado Boulder, Boulder, CO, USA
[4] NOAA Chemical Sciences Laboratory, Boulder, CO, USA

Corresponding authors: Aaron G. Meyer (agmeyer4@gmail.com), Manvendra K. Dubey (dubey@lanl.gov)

Key Points

- Multiple measurement techniques across spatiotemporal scales show consistent and stable ethane:methane ratios from a coal vent shaft
- Ethane:methane ratios are a valuable tool for source apportionment, plume separation, and O&G basin emissions characterization
- A large gas plant source was identified in 2015 but abated in 2021 showing change with time and monitoring

This is the author manuscript accepted for publication and has undergone full peer review but has not been through the copyediting, typesetting, pagination and proofreading process, which may lead to differences between this version and the Version of Record. Please cite this article as doi: 10.1029/2022JD037092.

Abstract
Source attribution of natural gas emissions from fossil fuels in New Mexico's San Juan Basin (SJB) is challenging due to source heterogeneity and emissions transience. We demonstrate that ethane (C_2H_6) to methane (CH_4) mixing ratios can identify and separate sources over different scales using various measurement techniques. We report simultaneous CH_4 and C_2H_6 observations near a coal mine vent and oil and gas (O&G) emission sources using ground-based in situ measurements in 2020/2021. During these campaigns, we observed a stable coal vent C_2H_6:CH_4 ratio of 1.28% +/- 0.11%, discernibly different than nearby O&G source ratios ranging from 0.9%. to 16.8%. We analyze airborne observations of the SJB taken in 2014/2015 that exhibit similar coal vent ratios and further show the region's heterogeneity. We identify episodic O&G sources, including a gas plant source detected in 2014/2015 that is absent in our 2020/2021 data. We examine total column observations of C_2H_6 and CH_4 made in 2013 with a solar spectrometer and find a C_2H_6:CH_4 ratio of 1.3% +/- 0.4% for the coal vent. The stable and unique coal vent ratio relative to other O&G sources in the region is used to demonstrate that consistent attribution is possible using various measurement methods at multiple scales across many years. Finally, we demonstrate that using C_2H_6 as a proxy for fossil CH_4 inversions can inform detailed basin-scale inversions, provided we understand source specific changes in the C_2H_6:CH_4 ratio like we report in the SJB.

Plain Language Summary
Oil, gas, and coal production processes are known to emit methane, a potent greenhouse gas, and other hydrocarbon air pollutants. Attributing these emissions to specific anthropogenic fossil sources is challenging in the vast and variable infrastructure. Ethane is often co-emitted with methane and the ratio of ethane to methane in emission sources varies significantly with source types. By measuring this ratio with high sensitivity and accuracy, we can "fingerprint" gas sources by their unique ratio. We report simultaneous measurements of ethane and methane, and an empirical analysis of the ratio to demonstrate source specific attribution. Our varied measurement techniques spanning spatial scales (near-source ground, airborne, and remote sensing) were used to sample sources in New Mexico's San Juan basin over 8 years. Despite a diverse and changing emissions environment, ethane to methane ratios were successfully used to identify and apportion several sources across scales in space and time. Specifically, our measurements show consistent and stable ethane to methane ratios from a large coal vent source in the study region. Our findings inform efforts seeking to characterize and quantify gas emissions in fossil extraction regions using multi-scale data from diverse instruments.

1 Introduction

The global average concentration of atmospheric methane (CH_4) rose in 2021 to 1896 parts per billion (ppb) (Dlugokencky & NOAA/GML, 2022) at the largest measured annual rate of 17 ppb to more than 2.5 times greater than in 1750 (Dlugokencky et al., 2011). Since 1750, methane has contributed over 25% to the cumulative anthropogenic radiative forcing, making it second only to carbon dioxide (CO_2) as an anthropogenic greenhouse gas (Saunois et al., 2020). Atmospheric methane levels continue to rise, with equal contributions to this increase made by fossil, agricultural, and landfill sources (Hausmann et al, 2016; Jackson et al., 2020). Methane's high global warming potential, 11.8 +/- 1.8 year atmospheric lifetime (IPCC, 2021), and value as a commodity indicate that emissions reductions offer a cost-effective strategy for near- to intermediate-term climate mitigation (Ocko et al., 2021). Of the fossil resources, coal contributes

5.9% and oil and gas contribute 11.2% to the global methane budget in inventories (Saunois et al., 2020). However, some top-down global (Schwietzke et al., 2016), national (Miller et al., 2013) and regional (Barkley et al., 2021) estimates show that fossil methane emissions may be much higher than inventories suggest. The discrepancies and uncertainties between top-down estimates and bottom-up inventories reinforce the importance of continued atmospheric methane monitoring and accurate accounting.

Fossil natural gas is primarily CH_4, but contains other hydrocarbons such as ethane (C_2H_6) at various mixing ratios that depend both on fossil deposit composition and downstream processing procedures (Cardoso-Saldaña et al, 2019, 2021). The ratio of C_2H_6:CH_4 is therefore useful for the attribution of different individual natural gas sources such as well heads, compressor stations, storage tanks, coal bed off-gassing etc. that are vented or leaked to the atmosphere. This ratio has been empirically shown to be a valuable method for identifying source signatures using ground- (Hopkins et al., 2016; Roscioli et al., 2015; Yacovitch et al., 2014) and aircraft-based (Gentner et al., 2014; Peischl et al., 2013, 2018,2015; Smith et al., 2015; Yacovitch et al., 2014) in situ instruments, as well as total column remote sensing systems (Kille et al., 2019; Wunch et al., 2016). While these studies have examined C_2H_6:CH_4 ratios using the variety of techniques listed, we are unaware of investigations which directly compare the ability of these different measurement techniques to use C_2H_6:CH_4 ratios for source attribution across spatial (meter to 10s of kilometer) and temporal (seconds to hours resolution) scales. Recent top down inversion studies have used atmospheric C_2H_6 to isolate CH_4 fossil sources (Barkely et al., 2021) by assuming constant basin wide ratios. However, basin wide C_2H_6:CH_4 ratios have been shown to have increased with time in some basins confounding their use in inversions (Lan et al., 2019). We examine this spatio-temporal variability in the SJB that has a multitude of fossil natural gas sources.

This study focuses on the large scale (regional enhancement, on the order of 100's of square kilometers), total column methane hot spot that was discovered above Four Corners, USA using space and ground observations and was attributed to fossil fuel extraction, distribution, and use (Kort et al., 2014). Subsequent characterization campaigns (Frankenberg et al., 2016; Smith et al., 2017; Pétron et al., 2020) and satellite surveys (Varon et al., 2020) highlight a ventilation shaft, which services the San Juan coal mine, as a prominent source of CH_4. Other sources identified in the area include a plethora of oil and gas extraction, transport, storage, and processing facilities. These fossil fuel operations translate to potential emission sources which are heterogeneous in location, size, type, and vary with time (Frankenberg et al., 2016).

We specifically target the coal vent shaft as a known large point source of C_2H_6 and CH_4 to observe and analyze C_2H_6:CH_4 ratios for source identification using three different measurement techniques across eight years of data (2013-2021). In December 2020 and October 2021, we deployed a ground-based mobile station with in situ CH_4, C_2H_6, and 3-D sonic wind sensors to observe the local composition of the region. Our measurements are complemented by two airborne campaigns in 2014 and 2015 (TOPDOWN and SONGNEX) which measured C_2H_6 and CH_4 from targeted sources, including the coal vent shaft (Smith et al., 2017). Finally, we used a ground-based solar Fourier transform spectrometer (FTS) (Lindenmaier et al., 2014) to observe total column C_2H_6 and CH_4 in the region in March and September of 2013.

We report a stable and unique C_2H_6:CH_4 ratio of approximately 1.3% from the coal vent plume during all three campaigns across spatial (from meters scale for mobile transects to kilometers scale for total column measurements) and temporal (second resolution for mobile transects to minutes/hours resolution for total column measurements) scales. Both the ground-based mobile and aircraft campaigns illustrate the highly heterogeneous and transient emissions landscape in the region, a critical issue in using C_2H_6 to infer CH_4 emissions from O&G basins (Barkley et al., 2021; Lan et al., 2019; Tribby et al., 2022). Despite the presence of other large and fluctuating hydrocarbon sources in the SJB, we were able to isolate and identify the coal vent plume using the C_2H_6:CH_4 ratio in each measurement campaign. Furthermore, plumes detected with mixed source origins showed ratios between those of their origin sources, indicating the possibility of developing empirical linear mixing rules for source attribution, and the diagnostic value of the intensive (quantity independent) C_2H_6:CH_4 ratio for plume mixing. We suggest that our results in the SJB provide a basis for source identification and apportionment using a variety of measurement techniques that can be extended to other oil and gas basins to inform source inversions.

2 Methods

2.1 Field Site

The San Juan Basin in the Four Corners region of New Mexico is primarily badlands type terrain featuring buttes, mesas, drainages, sparse vegetation, and complex topography. There are extensive coal deposits, natural seeps, vent shafts, coal bed methane, two large power plants (Lindenmaier et al., 2014), and O&G operations. Recent campaigns have probed the multitude of CH_4 and C_2H_6 emission sources associated with the large coal mine and other oil and natural gas operations in this region (Frankenberg et al., 2016; Pétron et al., 2020). These potential emission sources include extraction wells, transmission pipelines, storage facilities, compressor stations, and processing plants, among others.

2.1.1 Coal Vent Shaft

One of the largest CH_4 sources in the Four Corners region is the ventilation shaft located at 36.7928°N, 108.3890°W, hereafter referred to as the "coal vent", which services the longwall subsurface San Juan coal mine (United States Department of Interior, 2018). Estimates of CH_4 emission fluxes from the coal vent range from 360 to 2800 kg/h as reported by multiple aircraft campaigns (Frankenberg et al., 2016; Pétron et al., 2020), and EPA records (United States Environmental Protection Agency, 2019). Varon et al (2020) estimate emissions from the vent at 2390+/-1070kg/h using GHGSat-D satellite observations.

2.1.2 Natural Gas Plant

An additional source of CH_4 in the region is the San Juan River (SJR) natural gas plant located at 36.759°N, 108.366°W. The New Mexico Environment Department reported variable methane emissions between 2013 and 2020, ranging from approximately 4 to 50 kg/h (New Mexico Environment Department, 2021). The SJR plant was independently identified as a CH_4 source by both Frankenberg et al. (2016) and Pétron et al. (2020) using datasets collected in 2015. Additionally, a 2020 settlement found the SJR plant exceeded EPA pollution standards by flaring emissions including volatile organic compounds, carbon monoxide, nitrogen oxides, hydrogen sulfide, and sulfur dioxide, over a 761 day period from 2016-2018 (State of New Mexico, 2020).

A civil penalty of $950,000 was assessed, and the operator agreed to undertake a voluntary audit of the plant.

2.2 Sampling and Instrumentation

A variety of instruments have been used in studies to characterize methane emissions over large regions. Methane instruments include in situ surface networks, path integrated remote sensors, and satellites, each featuring distinct advantages and disadvantages, with the goal of capturing the heterogeneity in emissions (Wunch et al 2016, Cusworth et al., 2020). Such a multiscale monitoring approach has been successfully demonstrated to constrain emissions in large oil and gas (Harriss et al., 2015), urban (Wunch et al, 2016, Cusworth et al., 2020), and wetland (Hartley et al., 2015) regions. We apply and expand this multiscale monitoring framework by investigating C_2H_6, CH_4 and the C_2H_6:CH_4 ratio for source attribution in the SJB that is dominated by coal, oil and gas emissions.

2.2.1 Ground Based Mobile In Situ

A new and key component to this field study was gathering local (<5 km) in situ observations of gas plumes from various sources in the San Juan Basin. We extended novel technology capable of measuring CH_4 and C_2H_6 dry mixing ratios and 3-D winds simultaneously (Franco et al., 2016; Travis et al., 2020) to a mobile platform, hereafter referred to as the "mobile station". Dry CH_4 and C_2H_6 concentrations (<1 ppb accuracy) were gathered at 1Hz data rate using an Aeris (Hayward, CA) mid-IR spectrometer (PICO series). Horizontal and vertical wind data were collected at 5Hz data rate using an Anemoment (Longmont, CO) Trisonica Mini 3D anemometer. Location data were gathered using a Garmin 19x NMEA 2000 GPS Antenna.

We observed emission plumes at distances between 10m and 5 km using two sampling methods, stationary and moving plume transects, as described in SI Text S1 and shown in Figure 2. The mobile station enabled a fine scale survey of the study region as individual sources were located, sampled, and analyzed in real time. However, spatial coverage was limited by road access, wind conditions, and driving time.

2.2.2 Aircraft In Situ

Two aircraft campaigns conducted by NOAA provided airborne in situ data in the San Juan Basin. For this study, data were limited to the region enclosed by latitudes 36° to 37.5°N and longitudes 107.5° to 109°W. The TOPDOWN campaign, conducted from May–June in 2014 and April 2015 (TOPDOWN 2014), deployed a Twin Otter airplane. The instrument payload included measuring CH_4 with a cavity ringdown spectrometer (Picarro G2401-m) and C_2H_6 using an Aerodyne miniQCL tunable infrared laser direct absorption spectrometer (TOPDOWN 2014). The SONGNEX campaign in 2015 (SONGNEX 2015) deployed a Lockheed WP-3D Orion aircraft and measured CH_4 data using a Picarro cavity ringdown spectrometer, (G1301-m) and C_2H_6 data using an Aerodyne mini spectrometer . Each aircraft campaign flew patterns upwind, downwind, and circled sources of interest, producing plume transects similar to those collected by the mobile station. Aircraft data and instrument configurations are available at https://csl.noaa.gov/groups/csl7/measurements/ .

The aircraft-based campaigns offered much larger spatial coverage compared to the ground based mobile station, but were not capable of the fine scale characterization offered by a ground-

based unit. Additionally, field deployment of such aircraft campaigns is expensive, requiring extensive labor, foresight, and coordination.

2.2.3 Ground Based TCCON solar FTS with Mid-IR Detector

The Bruker 125HR (Bruker Optics, Germany) is a high-resolution solar Fourier transform spectrometer (FTS) designed to measure regional atmospheric column composition. This instrument was installed at the Four Corners site (36.798°N, 108.480°W) in March 2011 to make solar measurements in the near-infrared (NIR) spectral region for emissions verification purposes (Lindenmaier et al., 2014). This FTS was part of the Total Carbon Column Observing Network (TCCON), which has stringent protocols for operations, data analysis, and calibration that were established to ensure high accuracy and precision for total column CO, CO_2, CH_4, NO_2 and H_2O mixing ratio retrievals (Wunch et al., 2011). Trace gas retrievals were performed using spectra in the standard TCCON near-IR domain (3,800–15,500 cm^{-1}) with InGaAs (3,800–12,000 cm^{-1}) and Si-diode detectors (9,500–30,000 cm^{-1}). Additionally, we measured total column C_2H_6 using mid-IR spectra measured with a cryogenically (liquid N_2) cooled photovoltaic InSb (1,850–10,000 cm^{-1}) detector (Kille et al., 2017) in conjunction with a standard narrow bandpass filter which limits the wavenumber range of the spectra, thus increasing the signal-to-noise ratio. Interferograms were collected every three minutes, and the GGG2014 software distribution was used to retrieve the total column abundances of the atmospheric constituents mentioned above (Wunch et al., 2011, 2015; Toon, 2014). We observed absorption features of C_2H_6 at 2976, 2983 and 2986 cm^{-1} in the solar spectrum similar to Kille et al. (2017). We report total column abundances of CH_4 and C_2H_6 and focus our analysis on the C_2H_6:CH_4 ratios, thereby diminishing pressure or airmass correction factor effects. Total column C_2H_6 is an established method for fossil natural gas characterization, as described in Wunch et al. (2016). Thirteen total days of CH_4 and C_2H_6 data were collected during campaigns in March and September of 2013.

3 Results

This study focuses on comparing enhancement ratios of C_2H_6:CH_4 from well-defined point sources (Figure 1) for source attribution from three distinct data collection campaigns. The locations of the study region, campaigns, and emission sources of interest are shown in Figure 1. While other O&G operations are present in the region, those shown in Figure 1 represent known sources identified by Frankenberg et al (2016), Pétron et al (2020), or were found to be emitting methane by our mobile surveys in 2020/2021. No known agricultural or ruminant sources exist in the domain of Figure 1, and such sources outside the map domain are accounted for by subtracting regional background concentrations.We find that despite a highly heterogenous (both spatially and in source type) and transient emissions environment, specific sources, including the coal vent, can be identified by their C_2H_6:CH_4 ratios using different measurement techniques.

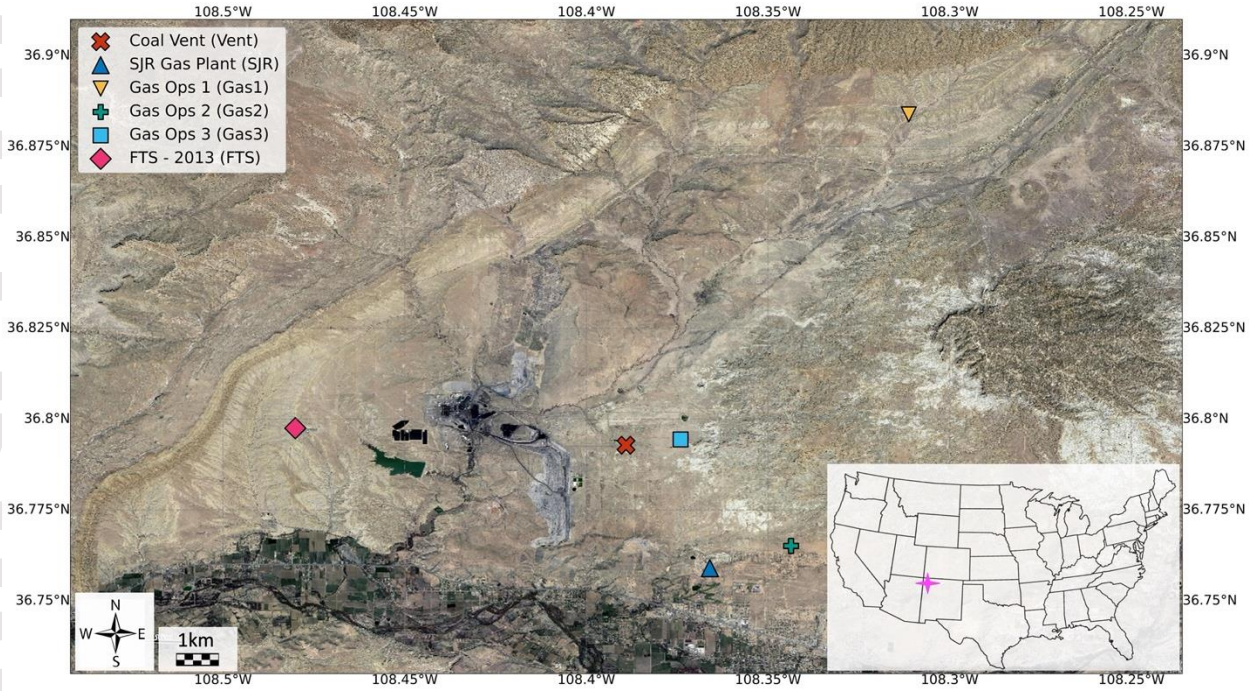

Figure 1. Map showing the San Juan, NM region containing a large coal mine. Known methane emission sources sampled during 2020/2021 mobile surveys and the location of the FTS instrument are identified.

3.1 Mobile Station (2020-2021)

An illustrative snapshot of our data in Figure 2 shows both stationary data capture and moving transects of the coal vent plume, expatiated in SI Text S1. Figure 2b and Figure 2c demonstrate the slowly changing regional background, which is subtracted in the calculation of excess CH_4 and C_2H_6 and explained in SI Text S2. Parallel linear regressions in Figure 2c show that coal vent plume transects exhibit similar ratios, despite differences in absolute concentrations caused by the background. Regressions shown in this and future sections are Model II linear regressions to account for measurement error in both CH_4 and C_2H_6. However, due to low relative error in measurements (<1 ppb) and the size of plume signals, the difference between Model II and typical Model I ordinary least squares regressions is negligible.

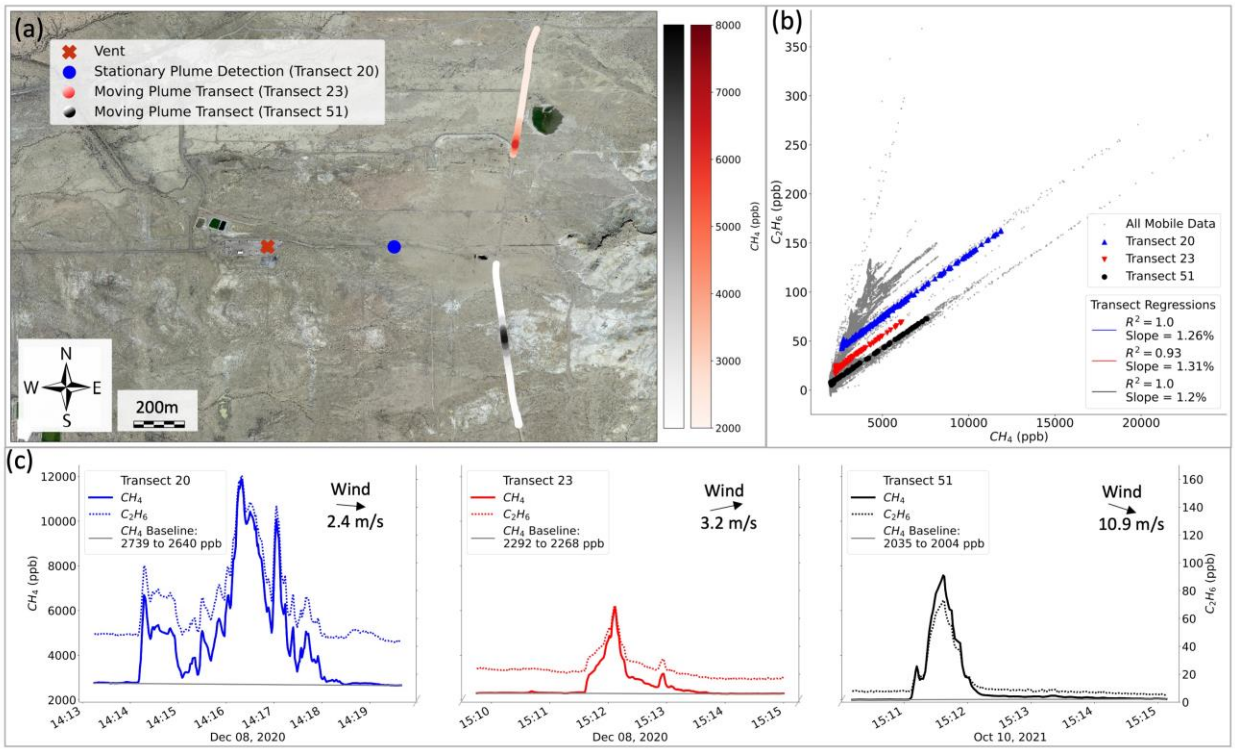

Figure 2. Three example transects of the coal vent plume. (a) Map illustrating three plume transects, one stationary "meteorological" transect (blue – 20), and two traditional transects (red –23, black/white – 51). (b) C_2H_6:CH_4 scatter and ratio. All other mobile data is shown in grey, and the three example plumes with their associated linear regression statistics are highlighted. (c) CH_4 and C_2H_6 timeseries plots of each example plume. Baseline values of CH_4 (pre- to post- plume minima) are shown as a solid grey line and change based on transect time and wind conditions, which is also seen in the C_2H_6 data.

Identification of the coal vent plume was generally straightforward using observed wind direction and source location. The study area also features a variety of other intermittent sources with distinct C_2H_6:CH_4 ratios. Figure 3 (and associated map in Figure 1) shows four such identified point sources: the coal vent and three different natural gas operation facilities. Despite their relatively close proximity (<5 km), these sources had markedly different C_2H_6:CH_4 ratios, ranging from the coal vent's stable ~1.3% ratio, to as high as ~14% from one of the gas facilities.

Figure 3 also illustrates two methods for calculating the C_2H_6:CH_4 ratio, point-by-point (a) and linear regression (b). When the station is sampling a plume, the point-by-point ratios become stable and match the ratios in the regression plot. To illustrate this, we filter the example data from Figure 3 to points where the excess CH_4 is greater than 50% of the maximum plume concentration, indicating strong plume sampling and diminishing the effects of rapidly rising and falling concentrations at plume edges. The point-by-point ratios during these times of strong plume detection are then compared with the linear regressions and shown in Table 1.

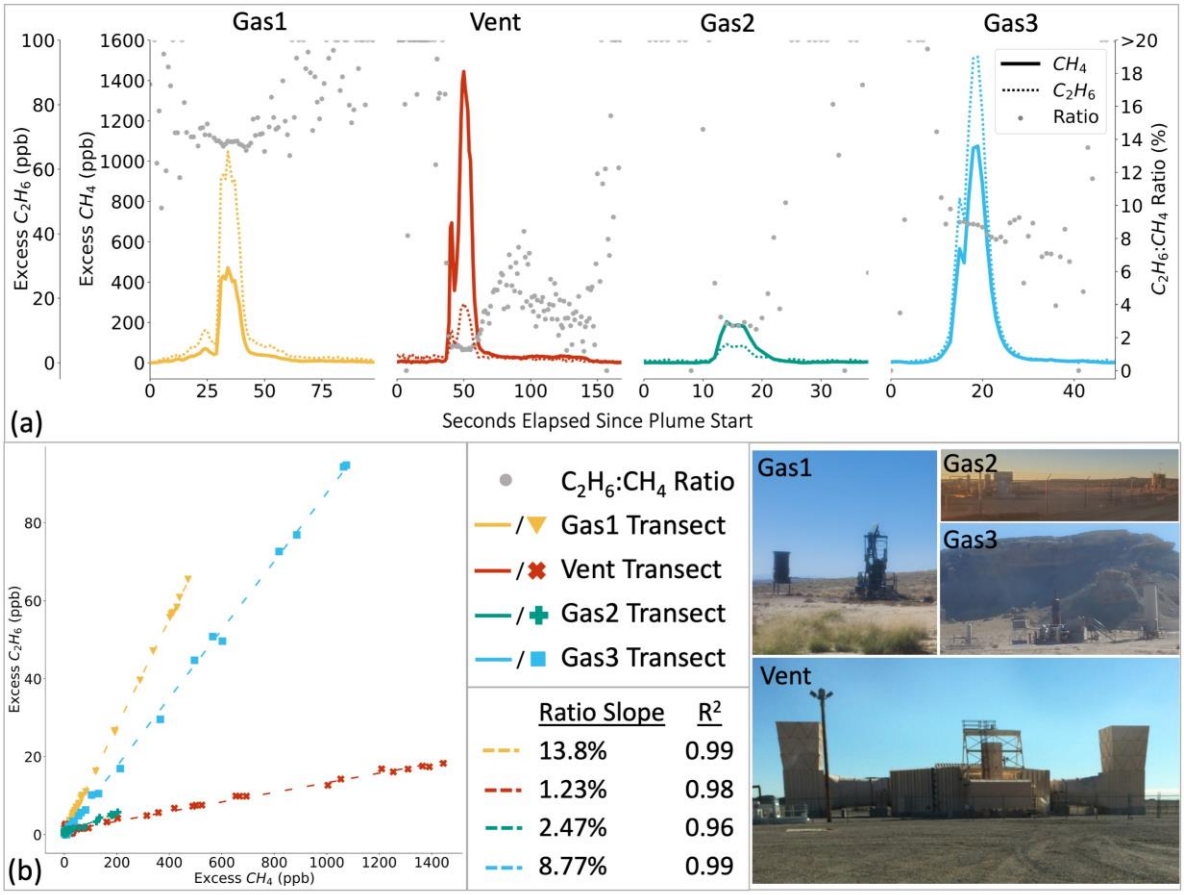

Figure 3. Mobile station data from four different source plumes. (a) Timeseries for four plumes. Solid lines show the excess CH_4 concentration (above background), dotted lines show excess C_2H_6 concentrations, and grey dots show the point-by-point C_2H_6:CH6 ratio, calculated using excess concentrations. (b) Scatter plot and corresponding linear regressions for each of the source plumes. Photos of each source shown in lower right. Source locations are shown in Figure 1.

Table 1: Regression Ratios Compared with Point-By-Point Ratios for Plumes in Figure 3

Source ID	Regression Ratio, R^2	Point-By-Point Ratio Mean	Point-By-Point Ratio STD
Gas1	13.8%, 0.99	13.8%	0.1%
Vent	1.23%, 0.98	1.29%	0.05%
Gas2	2.47%, 0.96	2.85%	0.2%
Gas3	8.77%, 0.99	8.75%	0.2%

The different source ratios are “fingerprints” that allow for the identification of sources without the need for wind data or transport modeling to infer source origin, provided known and consistent emission ratios such as those seen in the data presented here. Thus, point-by-point ratios provide a method for separating and identifying sources of excess CH_4 in real time using only the C_2H_6:CH_4 ratio, without the need for regression. Even in a highly transient and variable

emissions environment like our study area, different sources are quickly and easily identified using the ratio.

In total, we conducted 68 mobile transects in the region from 36.6° to 36.9°N and 107.9° to 108.5°W. Using ratios as fingerprints and associated geolocation, we identified 12 different sources with C_2H_6:CH_4 ratios ranging from 0.9% to 16.8%. In aggregating the coal vent data, we use transects where the C_2H_6:CH_4 ratio regression exhibits R^2>0.9, indicating strong sampling of the coal vent plume and little mixing from other sources. One outlier with a total plume ratio of 1.6% is shown in Figure S5 and Text S5. This longer "meteorological transect" sampled plume edges that increased the ratio. Subsampling the core of this plume results in a slope of 1.37% indicating that the bias may come from other source influence, rather than a changing vent ratio (Figure S5). In total sampled the coal vent 37 times and found a C_2H_6:CH_4 ratio of 1.28% +/- 0.11% (mean +/- 1 standard deviation) and SI Figure S4 shows the probability density function of these 37 transects that is a normal distribution. The low relative standard deviation indicates temporal stability over the measurement periods, both during campaigns (hours-days) and between campaigns (10 months). We suggest that this stability indicates a constant ratio associated with coal-bed off-gassing in this particular reservoir.

The SJR plant, which was identified in previous studies (and further examined in Section 3.2) as a significant CH_4 emissions source, was surveyed by the mobile station in October 2021. This survey showed CH_4 less than 500 ppb above background when sampled at close (<0.5 km) range in low wind (<4m/s) conditions. Concentrations of C_2H_6 were indistinguishable from background, and C_2H_6 was poorly correlated (<0.1 R^2) with CH_4, unlike other detected plumes.

3.2 Airborne Campaigns (2014, 2015)

The larger spatial coverage of the aircraft flights allowed multiple source plumes to be sampled in single subregional transects, as shown in Figure 4. This example transect illustrates the effectiveness of using the empirical C_2H_6:CH_4 ratio to identify plume origin. By plotting the point-by-point ratio as described in section 3.1, we identify three distinct plume regimes with ratios of ~2.5%, ~1.3%, and ~6–8%. These three regimes correspond with three separate origins: the SJR plant, coal vent, and smaller mixed regional gas operations, with peak excess CH_4 signals of 137, 492, and 25 ppb, respectively. We note that while the Gas1-Gas3 sources shown in Figure 1 have been included in Figure 3b, none of these sources were identified by Frankenberg et al. (2016) or Pétron et al. (2020), whose analysis used data from the same time period. This underscores the transient nature of emission flux from oil and gas operations.

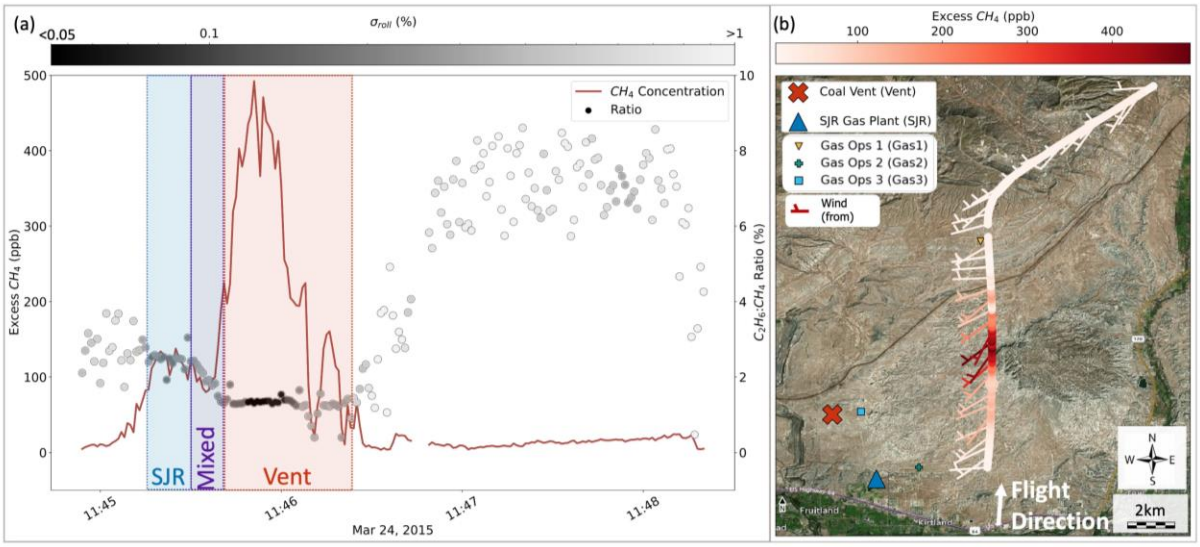

Figure 4. Example flight transect of the coal vent, SJR plant, and northern gas operation plumes. (a) Timeseries of the transect with CH_4 concentrations shown as a line, and point-by-point ratio shown as points. Ratio points are colored by the standard deviation of the ratio in a 10 second rolling window surrounding each point. The SJR and vent plumes are highlighted in light blue and red, respectively and the mixed regime in purple. (b) Map of the transect, flying south to north, colored by CH_4 concentration. Wind barbs indicate wind direction (blowing from). Average wind speed during transect was 4.4m/s.

Effective atmospheric modeling of the sources requires accurate dispersion parameters such as boundary layer height, topography, wind conditions, and source flux estimates. To explore the potential of using such a tool, we examine the plumes in Figure 4 using a simple steady-state Gaussian plume model (Seinfeld & Pandis, 2006) shown in SI section S6. Our gaussian plume simulations are very sensitive to parameter values for wind, stability, and boundary layer height and model results span a large range that includes our observations. We conclude that comprehensive measurements of meteorological conditions are needed to model source dispersion accurately for comparison with our data that are beyond the scope of this study. While modeling may be a valuable tool in certain situations, valuable source apportionment information can be obtained using the C_2H_6:CH_4 ratio without the need for dispersion modeling. Furthermore, Figure 4 and Figure S6 show that the C_2H_6:CH_4 ratio changes when plumes mix in both empirical and modeled data. This illustrates the value of using C_2H_6:CH_4 ratio as an intensive property to constrain plume mixing.

We extend the point-by-point ratio analysis in Figure 4 to include a rolling standard deviation of the ratio (σ_{roll}) as a measure of stability in the ratio. This parameter is defined as the standard deviation of the C_2H_6:CH_4 ratio in a 10 second window centered around each point. In this formulation, low σ_{roll} values represent periods during which the ratio is relatively constant in the timeseries, indicating good plume detection and a ratio usable for source identification. The transect in Figure 4 illustrates two periods of low σ_{roll} (during detection of the SJR plant and coal vent), one period of moderate σ_{roll} (during detection of variable gas operations further north), and multiple periods of high σ_{roll}, indicating no plume detection (excess CH_4 values close to zero).

A summary of the data collected from the San Juan Basin region during the TOPDOWN and SONGNEX aircraft campaigns is shown in Figure 5 alongside our mobile station data taken seven years later to facilitate comparison. The wide range of slopes in both plots confirms the high degree of heterogeneity in C_2H_6:CH_4 ratios in both data sets. As the aircraft data probed a wider array of sources at larger scales than our targeted mobile sampling at close distance, the excess CH_4 is larger and the plumes clearer in the latter. Despite the complex heterogeneity, low σ_{roll} values identify points during which plumes were intact and ratios were stable. Most notably, many low σ_{roll} values fall along the lines with ratios equal to that of the coal vent, indicating an intact plume, and a ratio that is consistent in both the aircraft and mobile data supporting a stable composition of the emissions. We note three other prominent plumes in the mobile data of Figure 5. Gas3 is the source identified in Figure 3. "Other" is a plume from an unknown gas operation, but is not associated with the SJR plant, as its location is far from the SJR plant. Our mobile station sampled close to the SJR plant in 2020 and 2021 and did not show elevated methane levels, further illustrated on the right side of Figure 5 (no points in the SJR ratio range).

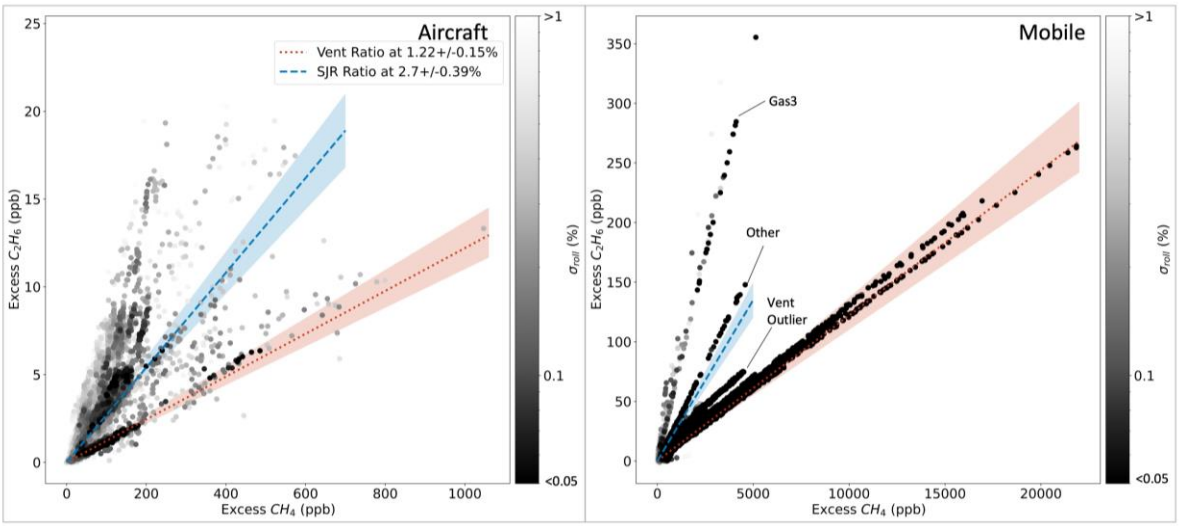

Figure 5. Aircraft plume data from the San Juan Basin measured during TOPDOWN and SONGNEX campaigns, and mobile station plume transect data measured in 2020/2021. Points are colored by σ_{roll} (log scale, 10 second window, 5 point per window minimum), indicating periods when the aircraft was detecting a plume with a constant ratio. Ratios of the SJR plant and coal vent are shown as dotted lines (standard deviation shaded) on both plots, showing the intact plumes detected at these ratios. Prominent mobile plumes are labeled.

Using these ratios for source identification, in conjunction with inferred transport using wind data, we identified over 200 discrete plume transects spanning 12 flight days in the region. Of these plume transects, we identified over 50 sources with ratios ranging from 0.2% to 21.8%. The SJR plant was sampled 7 times, with a ratio of 2.69% +/- 0.39% (mean +/- 1 standard deviation). The coal vent plume was sampled 14 times, with a ratio of 1.22% +/- 0.15%.

While the ratio is useful for plume separation in scenarios like that presented in Figure 4, it can also be a diagnostic for plume mixing. We identify 11 periods of sampling during which the SJR plant and coal vent plumes were indistinguishable using their ratio due to plume mixing, meteorologic conditions, and transect locations. During these 11 "mixed plume" events, we find a ratio of 1.89% +/- 0.35%. As the ratio is an intensive, observable quantity, it could be used to

quantify source mixing on a weighted mass flux basis. This would require accurate dispersion and source flux parameters whose collection is beyond the scope of this study. Mixed plume event details and further discussion can be found in SI Text S3 and Figure S2, and an illustration of how ratios coupled with modeling may be feasible is shown in SI Text S6, and Figures S6-S8.

The results presented here agree with those from the mobile station results. Specifically, we find that sources can be separated and attributed using point-by-point C_2H_6:CH_4 ratios, even in a region with complex emissions. We highlight the discovery that despite the broader spatial scale and different measurement years between the aircraft and mobile measurements, the techniques provided similar results and the coal vent ratio remained constant. Furthermore, we underscore the presence of the SJR plant plume in the aircraft data. This plume was not detected during the 2020/2021 mobile surveys as described in Section 3.1, and its absence may be related to the 2020 settlement and subsequent self-audit of this facility (State of New Mexico, 2020).

3.3 Total Column CH_4 and C_2H_6 Solar FTS Observations (2013)

Unlike the in situ measurements collected using the mobile and aircraft stations, the FTS instrument measures the total atmospheric column abundance of gas species. It is therefore less sensitive to local fluxes and more representative of regional CH_4 emissions (Lauvaux & Davis, 2014; Keppel-Aleks et al., 2011) that are also monitored by satellites and used for inversions (Kort et al, 2014; Turner et al, 2015). We gathered total column C_2H_6 and CH_4 data on 13 days in 2013, six in March and seven in September, in the SJB and use it to illustrate the value of large scale remote observations of the ratios. Our solar-FTS site was located approximately 8 km west of the coal vent (Figure 1), a distance ill-suited for ground-based in situ plume detection but apropos for total column measurement.

Most mornings, easterly winds bring air from the coal vent, producing a fairly stable C_2H_6:CH_4 ratio of approximately 1.3%, shown in Figure 6. As winds shift to southerly around 11:00 local time, and eventually westerly around 14:30 local time, C_2H_6 and CH_4 column abundances drop. During this wind shift, the C_2H_6:CH_4 ratio drops as well, illustrating the absence of a strong source ratio from the measured airmass.

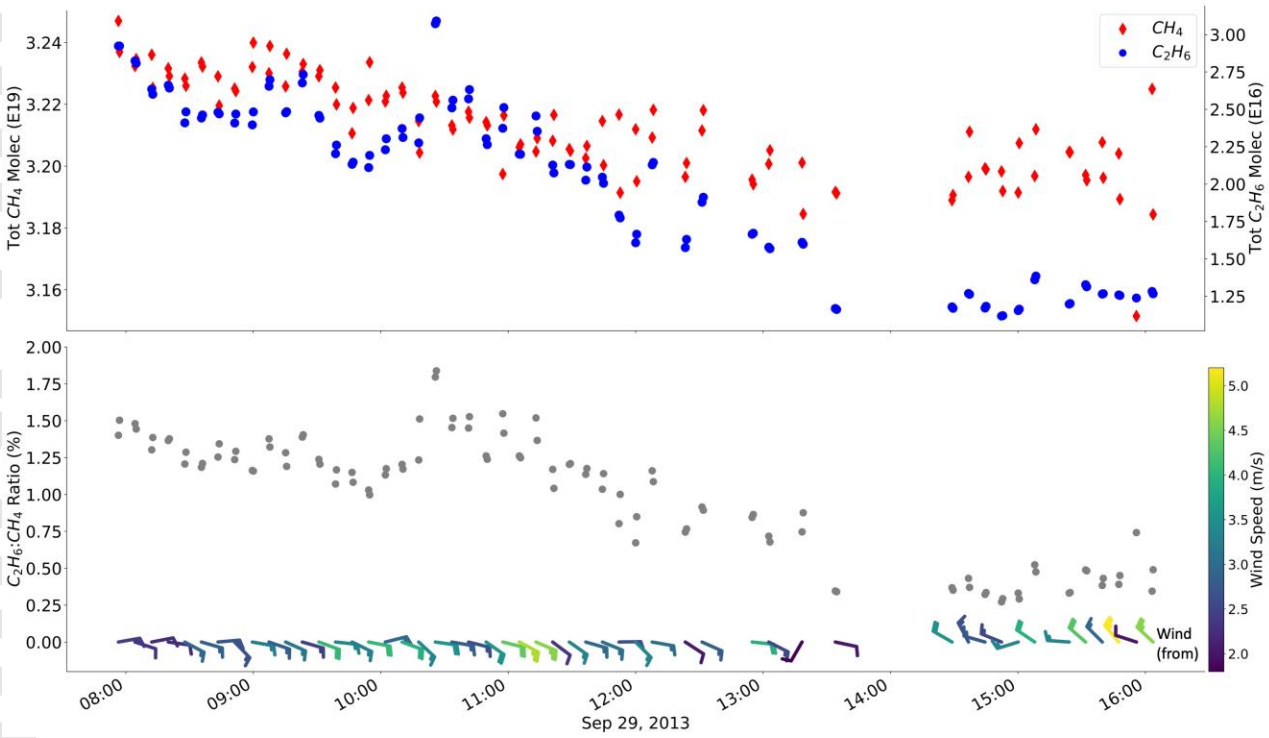

Figure 6. Example FTS data for a typical day. Total column abundances for CH_4 (blue) and C_2H_6 (red) and point-by-point C_2H_6:CH_4 ratios are shown in the top and bottom panels, respectively. Wind barbs representing the direction wind is blowing from, colored by wind speed, are shown at the bottom. Winds shift from easterly to westerly near midday, causing a large drop in ethane and C_2H_6:CH_4 ratio.

In an aggregation of the FTS data, data points were binned by wind direction and plotted as a pollution rose (Figure 7), showing the C_2H_6:CH_4 ratio (calculated using excess concentrations) in each bin.

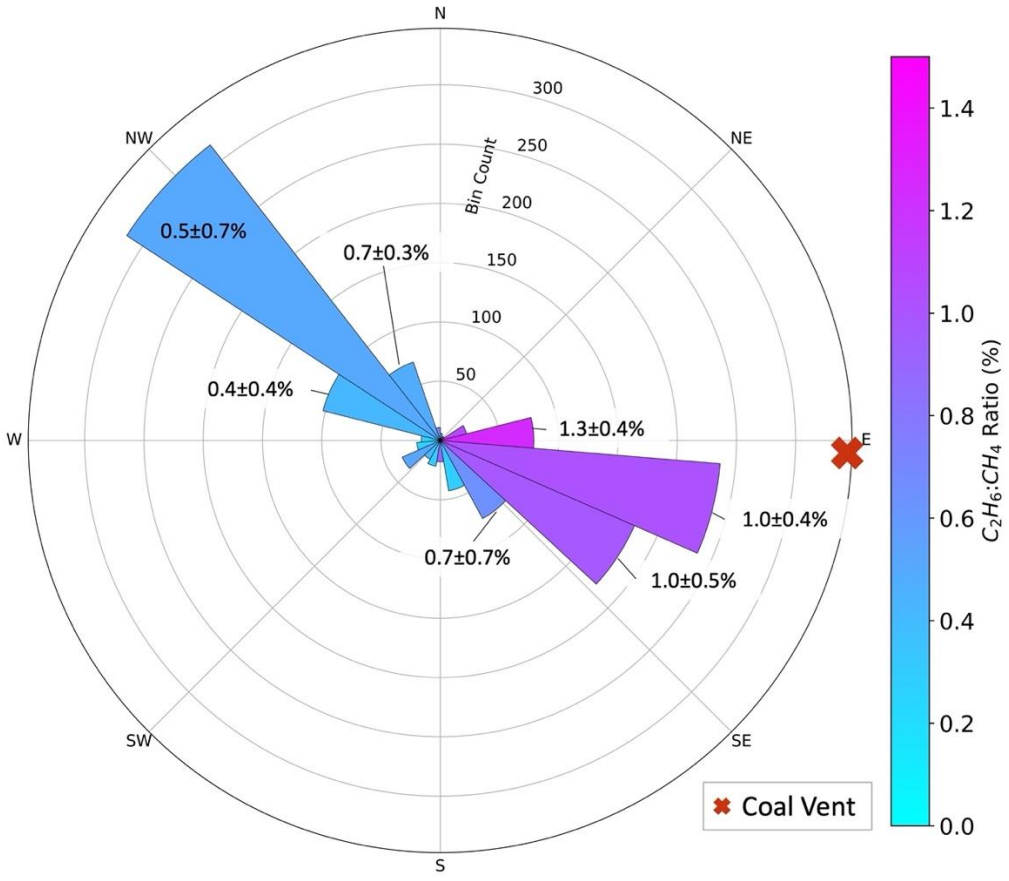

Figure 7. Pollution rose centered at FTS station. All data from FTS is separated into wind direction bins on the θ axis, and the number of observations in each bin is shown on the radial axis. Each bin has an associated excess C_2H_6:CH_4 ratio and error, representing the mean and standard deviation (respectively) of the point-by-point ratios in each wind direction bin.

When the wind is blowing from the coal vent, the mean excess column abundance ratio is 1.3+/-0.4%, which matches 1.28+/-0.11% and 1.22+/-0.15% ratios from the in situ mobile and aircraft measurements, respectively. Furthermore, the wind direction bin containing the coal vent shows the lowest ratio standard deviation (relative to its value) compared with other bins, indicating a more consistently detectable ratio in this direction. When wind is not east/southeasterly, we observe ratios less than 1%, with high relative standard deviations. This is consistent with the assumption that fewer C_2H_6/CH_4 sources exist in these regions.

Our directional analysis coupled with the C_2H_6:CH_4 ratio observed in the total column abundances can be used to attribute and identify sources in the directions of interest. While the FTS measurements differ from in situ mobile and aircraft measurements both spatially (regional vs. local/subregional sensitivities), and temporally (longer term – hours), these FTS measurements are able to identify the consistent and unique 1.3% ratio from the coal vent.

4 Discussion

Oil and gas fields with a diverse array of fossil fuel operations pose a challenge for methane and hydrocarbon source apportionment. The San Juan Basin in the Four Corners is one such region,

representing the largest CH_4 regional anomaly in the United States (Kort et al., 2014; Pétron et al., 2020). This study addressed the challenge of discriminating and attributing specific CH_4 sources from a myriad of coal, oil, and gas activities in a subsection of the San Juan Basin by gathering simultaneous C_2H_6 and CH_4 observations.

While many studies have examined C_2H_6:CH_4 ratios using specific measurement techniques (Gentner et al., 2014; Hopkins et al., 2016; Kille et al., 2019; Peischl et al., 2013, 2018; Roscioli et al., 2015; Smith et al., 2015; Wunch et al., 2016; Yacovitch et al., 2014) this study provides a unique dataset allowing intercomparison between measurement techniques that are sensitive to different spatial and temporal scales. As more studies (Lan et al, 2019; Barkley et al, 2021; Tribby et al., 2022) investigate using C_2H_6:CH_4 and other hydrocarbon ratios to characterize basins and do methane emissions inversion, a "telescoping" approach that leverages measurements on different scales is a valuable characterization tactic. By illustrating our consistent ability to apportion sources using the C_2H_6:CH_4 ratio across measurement techniques and sensitivity scales, we provide a basis for future studies aiming to use satellite, other remote sensing, aircraft, and mobile in situ measurements in concert to characterize and apportion O&G emission sources.

4.1 Ratio Heterogeneity

Past research demonstrates that C_2H_6:CH_4 ratios found in fossil fuel extraction, processing, and transportation operations are highly variable (Cardoso-Saldaña et al., 2021; Peischl et al., 2018; Roest & Schade, 2017; Roscioli et al., 2015; Smith et al., 2015). Our findings confirm these highly variable C_2H_6:CH_4 source ratios in the field. This ratio heterogeneity has implications on recent efforts that use C_2H_6 as an independent proxy to determine oil and gas CH_4 emissions over North America. Barkley et al. (2021) use C_2H_6 observations convolved with a priori C_2H_6:CH_4 ratio maps to infer CH_4 emissions from fossil fuel operations. These C_2H_6:CH_4 ratio maps are spatially coarse as shown in SI Figure S2 of Barkley et al. (2021), which prescribes the San Juan Basin's C_2H_6:CH_4 ratio as >10%. Our results suggest that ratio heterogeneity from the mixing of sources, particularly the large coal vent with a low 1.3% ratio, underscores Barkley et al.'s (2021) conclusion that more detailed and accurate C_2H_6:CH_4 ratio maps would yield better methane flux inversions. Further observations of C_2H_6:CH_4 ratios in methane emitting regions, such as this study, will help achieve this.

4.2 Stable Coal Vent Ratios

Within this complex emissions landscape, the large coal vent shaft stood out as a source with a stable 1.3% C_2H_6:CH_4 ratio, which is consistent with the finding of a ~1.4% ratio from coal bed methane in Table 3 of Roscioli et al. (2015). The stability of the coal vent source, an important finding, allowed us to directly compare how three different data collection campaigns can identify the coal vent using the ratio. Table 2 summarizes the coal vent plume ratios calculated during each campaign. These results illustrate the stability of, and a consistent ability to detect, the coal vent ratio across measurement campaigns.

Table 2. Summary of campaigns. Discrete source count and range of ratios are excluded from FTS data due to the inability of the FTS to identify individual plumes.

Campaign	Dates	Measurement Type	Discrete Sources Detected	Range of Ratios in Detected Sources	Coal Vent Plume Ratio
Mobile	12/2020 – 10/2021	Ground-based in situ	12	0.9% – 16.8%	1.28 ± 0.11%
Aircraft	06/2014 – 04/2015	Aircraft-based in situ	>50	0.2% – 21.8%	1.22 ± 0.15%
FTS	03/2013 – 09/2013	Ground-based total column	n/a	n/a	1.3 ± 0.4%

4.3 Ratio Methods for Source Apportionment

Use of the C_2H_6:CH_4 ratio for source identification is not new (Gentner et al., 2014; Hopkins et al., 2016; Kille et al., 2019; Peischl et al., 2013, 2018; Roscioli et al., 2015; Smith et al., 2015; Wunch et al., 2016; Yacovitch et al., 2014); however, these studies typically calculate linear regressions between C_2H_6 and CH_4 and represent the ratio using the calculated slope. In contrast, we also calculate the ratio on a point-by-point basis, which provides results consistent with traditional regression techniques as shown in Figure 3 and Table 1.

This point-by-point method offers the additional advantage of time series-based source attribution, illustrated in Figure 4. When plotted using regression techniques, the aircraft plume in Figure 4 shows skewed or multiple slopes (Figure S4) due to the confluence of sources contributing to different parts of the plume. However, using the point-by-point method, the origin of excess CH_4 within the plume is elucidated, as the ratio quickly transitions from 2.5% (SJR plant) to 1.3% (coal vent) to 6–8% (gas operations). In cases where plumes are relatively unmixed and have discernable ratios, the intensive point-by-point ratio values can differentiate sources empirically; therefore, the need for local wind data, transport criteria, or modeling becomes less critical in identifying source origin.

We observed situations when sources become mixed during sampling, as diagnosed by the C_2H_6:CH_4 ratio values. This effect is most easily seen in specific aircraft transects (SI Figure S2) which sample airmasses with contributions from both the SJR plant and coal vent. We anticipate that source attribution may be possible using mass flux weighted linear mixing rules; however, this requires source flux, distance, and plume dispersion data beyond the scope of this study. Future work may be able to use the intensive C_2H_6:CH_4 ratio and develop mixing regimes such that even samples with mixed source origins can be used for separation and apportionment, a potentially valuable tool for emissions verification purposes.

4.4 Time Dependence of Emissions

Another key outcome of this study was the discovery of a sharp decline in emissions from the SJR plant in 2020/21. During the aircraft campaigns of 2014 and 2015 the SJR plant was identifiable, with a ratio of approximately 2.7% and maximum detected plume concentrations (during transects at similar distances and under similar wind conditions) on the same order as

those detected from the coal vent. However, multiple mobile surveys during our 2020 and 2021 campaigns did not detect a plume from the SJR plant.

This temporal change in emissions, coupled with the displayed spatial heterogeneity of ratios, is important in characterizing basins using C_2H_6:CH_4 ratios. Lan et al. (2019) studied long term measurements of C_2H_6 and CH_4 to conclude that basin-wide emission ratios are neither spatially uniform nor constant in time. Our case study shows the spatial heterogeneity empirically. The 1.3% coal vent ratio did not change between 2013 and 2021; however, any change in emission flux from the multitude of sources would affect a basin-wide value for C_2H_6:CH_4 ratio. Therefore, more detailed studies of C_2H_6:CH_4 ratios within emitting basins like this study are important for accurately inferring O&G emission trends.

5 Conclusion

In this study, we identified a multitude of previously identified sources (Frankenberg et al., 2016; Smith et al., 2017; Pétron et al., 2020), as well as new sources using C_2H_6:CH_4 ratios in the SJB. We demonstrated temporal stability of the C_2H_6:CH_4 ratio from a large source of coal bed natural gas over 8 years. Finally, we compared different measurements across scales (ground-based mobile in situ, aircraft-based in situ, and ground-based total column) to show that C_2H_6:CH_4 ratios can be used for source identification. Our findings indicate that despite differences in spatial and temporal scale, the C_2H_6:CH_4 ratio identified the coal vent source in each measurement campaign, even in a complex and heterogenous emissions environment.

This study illustrates the advantages of using C_2H_6:CH_4 ratios for source identification. We therefore suggest that a multiscale approach leveraging the advantages of these different measurement techniques, coupled with use of the C_2H_6:CH_4 ratio, may be a valuable practice for monitoring large, heterogeneous emissions environments. Our study highlights the value of synthesizing regional scale observations using a variety of techniques and platforms, each with specific strengths, to attribute greenhouse gas emissions (Wunch et al 2016, Cusworth et al 2020). Extending our method to other oil and gas basins, including those with large biogenic sources that do not emit any C_2H_6 will be valuable for source inversions.

Acknowledgments

This study was funded under the University of California Office of the President's Grant LFR-18-548581. Solar FTS measurments were supported by the LANL Laboratory Directed Research and Development (LDRD) project "Multi-Scale Science Framework for Climate Treaty Verification: Attributing & Tracking GHG Fluxes Using Co-Emitted Signatures". We would like to acknowledge Geoff Toon for his assistance in FTS data processing, especially in helping identify the spectral lines of ethane. We thank Kyle Gorkowski for proofreading and figure tuning. We also thank all those involved in the NOAA TOPDOWN and SONGNEX aircraft campaigns for their work in data collection, processing, and publication for our benefit. We specifically acknowledge Tom Ryerson for his involvement in the SONGNEX campaign, and Colm Sweeney and Anna Karion for providing methane measurements from TOPDOWN that are publicly available.

Open Research

Ground-based mobile in situ data, FTS retrievals, and associated weather data are publicly available at https://doi.org/10.17632/hwp3d8ghp2.1 (Meyer & Lindenmaier 2022). Aircraft data are available at https://csl.noaa.gov/projects/songnex/ for SONGNEX (SONGNEX 2015) and https://csl.noaa.gov/groups/csl7/measurements/2014topdown/ for TOPDOWN (TOPDOWN 2014).

References

Barkley, Z. R., Davis, K. J., Feng, S., Cui, Y. Y., Fried, A., Weibring, P., et al. (2021). Analysis of oil and gas ethane and methane emissions in the southcentral and eastern United States using four seasons of continuous aircraft ethane measurements. *Journal of Geophysical Research: Atmospheres, 126*(10). https://doi.org/10.1029/2020jd034194

Cardoso-Saldaña, F. J., Kimura, Y., Stanley, P., McGaughey, G., Herndon, S. C., Roscioli, J. R., et al. (2019). Use of light alkane fingerprints in attributing emissions from oil and gas production. *Environmental Science & Technology, 53*(9), 5483-5492. https://doi.org/10.1021/acs.est.8b05828

Cardoso-Saldaña, F. J., Pierce, K., Chen, Q., Kimura, Y., & Allen, D. T. (2021). A searchable database for prediction of emission compositions from upstream oil and gas sources. *Environmental Science & Technology, 55*(5), 3210-3218. https://doi.org/10.1021/acs.est.0c05925

Chen, J., Viatte, C., Hedelius, J. K., Jones, T., Franklin, J. E., Parker, H., et al. (2016). Differential column measurements using compact solar-tracking spectrometers. *Atmospheric Chemistry and Physics, 16*(13), 8479-8498. https://doi.org/10.5194/acp-16-8479-2016

Cusworth, D. H., Duren, R. M., Yadav, V., Thorpe, A. K., Verhulst, K., Sander, S., et al. (2020). Synthesis of methane observations across scales: Strategies for deploying a multitiered observing network. *Geophysical Research Letters, 47*(7). https://doi.org/10.1029/2020gl087869

Dlugokencky, E. J., Nisbet, E. G., Fisher, R., & Lowry, D. (2011). Global atmospheric methane: Budget, changes and dangers. *Philosophical Transactions of the Royal Society A: Mathematical, Physical and Engineering Sciences, 369*(1943), 2058-2072. https://doi.org/10.1098/rsta.2010.0341

Dlugokencky, E., & NOAA/GML. (2022, January). Global CH_4 monthly means. Retrieved January 13, 2022, from gml.noaa.gov/ccgg/trends_ch4/

Franco, B., Mahieu, E., Emmons, L. K., Tzompa-Sosa, Z. A., Fischer, E. V., Sudo, K., et al. (2016). Evaluating ethane and methane emissions associated with the development of oil and natural gas extraction in North America. *Environmental Research Letters, 11*(4), 044010. https://doi.org/10.1088/1748-9326/11/4/044010

Frankenberg, C., Thorpe, A. K., Thompson, D. R., Hulley, G., Kort, E. A., Vance, N., et al. (2016). Airborne methane remote measurements reveal heavy-tail flux distribution in

Four Corners region. *Proceedings of the National Academy of Sciences, 113*(35), 9734-9739. https://doi.org/10.1073/pnas.1605617113

Gentner, D. R., Ford, T. B., Guha, A., Boulanger, K., Brioude, J., Angevine, W. M., et al. (2014). Emissions of organic carbon and methane from petroleum and dairy operations in California's San Joaquin Valley. *Atmospheric Chemistry and Physics, 14*(10), 4955-4978. https://doi.org/10.5194/acp-14-4955-2014

Harriss, R., Alvarez, R. A., Lyon, D., Zavala-Araiza, D., Nelson, D., & Hamburg, S. P. (2015). Using multi-scale measurements to improve methane emission estimates from oil and gas operations in the Barnett Shale Region, Texas. *Environmental Science & Technology, 49*(13), 7524-7526. https://doi.org/10.1021/acs.est.5b02305

Hartley, I. P., Hill, T. C., Wade, T. J., Clement, R. J., Moncrieff, J. B., Prieto-Blanco, A., et al. (2015). Quantifying landscape-level methane fluxes in subarctic Finland using a multiscale approach. *Global Change Biology, 21*(10), 3712-3725. https://doi.org/10.1111/gcb.12975

Hausmann, P., Sussmann, R., & Smale, D. (2016). Contribution of oil and natural gas production to renewed increase in atmospheric methane (2007–2014): Top–down estimate from ethane and methane column observations. *Atmospheric Chemistry and Physics*, 16(5), 3227-3244. https://doi.org/10.5194/acp-16-3227-2016

Heerah, S., Frausto- Vicencio, I., Jeong, S., Marklein, A. R., Ding, Y., Meyer, A. G., et al. (2021). Dairy methane emissions in California's San Joaquin Valley inferred with ground- based remote sensing observations in the summer and winter. *Journal of Geophysical Research: Atmospheres, 126*(24). https://doi.org/10.1029/2021jd034785

Hopkins, F. M., Kort, E. A., Bush, S. E., Ehleringer, J. R., Lai, C., Blake, D. R., & Randerson, J. T. (2016). Spatial patterns and source attribution of urban methane in the Los Angeles Basin. *Journal of Geophysical Research: Atmospheres, 121*(5), 2490-2507. https://doi.org/10.1002/2015jd024429

IPCC (2021). Climate Change 2021: The Physical Science Basis. Contribution of Working Group I to the Sixth Assessment Report of the Intergovernmental Panel on Climate Change. Cambridge University Press, Cambridge, United Kingdom and New York, NY, USA. https://doi.org/10.1017/9781009157896

Jackson, R. B., Saunois, M., Bousquet, P., Canadell, J. G., Poulter, B., Stavert, A. R., et al. (2020). Increasing anthropogenic methane emissions arise equally from agricultural and fossil fuel sources. *Environmental Research Letters, 15*(7), 071002. https://doi.org/10.1088/1748-9326/ab9ed2

Jones, T. S., Franklin, J. E., Chen, J., Dietrich, F., Hajny, K. D., Paetzold, J. C., et al. (2021). Assessing urban methane emissions using column-observing portable Fourier transform infrared (FTIR) spectrometers and a novel Bayesian inversion framework. *Atmospheric Chemistry and Physics, 21*(17), 13131-13147. https://doi.org/10.5194/acp-21-13131-2021

Keppel-Aleks, G., Wennberg, P. O., & Schneider, T. (2011). Sources of variations in total column carbon dioxide. *Atmospheric Chemistry and Physics, 11*(8), 3581-3593. https://doi.org/10.5194/acp-11-3581-2011

Kille, N., Baidar, S., Handley, P., Ortega, I., Sinreich, R., Cooper, O. R., et al. (2017). The CU Mobile Solar Occultation Flux instrument: Structure functions and emission rates of NH_3, NO_2 and C_2H_6. *Atmospheric Measurement Techniques, 10*(1), 373-392. https://doi.org/10.5194/amt-10-373-2017

Kille, N., Chiu, R., Frey, M., Hase, F., Sha, M. K., Blumenstock, T., et al. (2019). Separation of methane emissions from agricultural and natural gas sources in the Colorado Front Range. *Geophysical Research Letters, 46*(7), 3990-3998. https://doi.org/10.1029/2019gl082132

Kort, E. A., Frankenberg, C., Costigan, K. R., Lindenmaier, R., Dubey, M. K., & Wunch, D. (2014). Four corners: The largest US methane anomaly viewed from space. *Geophysical Research Letters, 41*(19), 6898-6903. https://doi.org/10.1002/2014gl061503

Lauvaux, T., & Davis, K. J. (2014). Planetary boundary layer errors in mesoscale inversions of column-integrated co2measurements. *Journal of Geophysical Research: Atmospheres, 119*(2), 490-508. https://doi.org/10.1002/2013jd020175

Lan, X., Tans, P., Sweeney, C., Andrews, A., Dlugokencky, E., Schwietzke, S., et al. (2019). Long- term measurements show little evidence for large increases in total U.S. methane emissions over the past decade. *Geophysical Research Letters, 46*(9), 4991-4999. https://doi.org/10.1029/2018gl081731

Lindenmaier, R., Dubey, M. K., Henderson, B. G., Butterfield, Z. T., Herman, J. R., Rahn, T., & Lee, S. (2014). Multiscale observations of CO2, 13CO2, and pollutants at four corners for emission verification and attribution. *Proceedings of the National Academy of Sciences, 111*(23), 8386-8391. https://doi.org/10.1073/pnas.1321883111

Meyer, A. G.; Lindenmaier, R. (2022), Dataset for San Juan Basin Ethane/Methane [Dataset]. *Mendeley Data, V1,* https://doi.org/10.17632/hwp3d8ghp2.1

Miller, S. M., Wofsy, S. C., Michalak, A. M., Kort, E. A., Andrews, A. E., Biraud, S. C., et al. (2013). Anthropogenic emissions of methane in the United States. *Proceedings of the National Academy of Sciences, 110*(50), 20018-20022. https://10.1073/pnas.1314392110

New Mexico Environment Department Emissions Analysis Tool. (2019). Retrieved September 02, 2021, from https://eatool.air.net.env.nm.gov/aqbeatool/

Ocko, I. B., Sun, T., Shindell, D., Oppenheimer, M., Hristov, A. N., Pacala, S. W., et al. (2021). Acting rapidly to deploy readily available methane mitigation measures by sector can immediately slow global warming. *Environmental Research Letters, 16*(5), 054042. https://doi.org/10.1088/1748-9326/abf9c8

Peischl, J., Eilerman, S. J., Neuman, J. A., Aikin, K. C., De Gouw, J., Gilman, J. B., et al. (2018). Quantifying methane and ethane emissions to the atmosphere from central and western U.S. oil and natural gas production regions. *Journal of Geophysical Research: Atmospheres*. https://doi.org/10.1029/2018jd028622

Peischl, J., Ryerson, T. B., Aikin, K. C., Gouw, J. A., Gilman, J. B., Holloway, J. S., et al. (2015). Quantifying atmospheric methane emissions from the Haynesville, Fayetteville, and Northeastern Marcellus Shale gas production regions. *Journal of Geophysical Research: Atmospheres, 120*(5), 2119-2139. https://doi.org/10.1002/2014jd022697

Peischl, J., Ryerson, T. B., Brioude, J., Aikin, K. C., Andrews, A. E., Atlas, E., et al. (2013). Quantifying sources of methane using light alkanes in the Los Angeles Basin, California. *Journal of Geophysical Research: Atmospheres, 118*(10), 4974-4990. https://doi.org/10.1002/jgrd.50413

Pétron, G., Miller, B., Vaughn, B., Thorley, E., Kofler, J., Mielke-Maday, I., et al. (2020). Investigating large methane enhancements in the U.S. San Juan Basin. *Elementa: Science of the Anthropocene, 8*(1). https://doi.org/10.1525/elementa.038

Roest, G., & Schade, G. (2017). Quantifying alkane emissions in the Eagle Ford Shale using Boundary Layer Enhancement. *Atmospheric Chemistry and Physics, 17*(18), 11163-11176. https://doi.org/10.5194/acp-17-11163-2017

Roscioli, J. R., Yacovitch, T. I., Floerchinger, C., Mitchell, A. L., Tkacik, D. S., Subramanian, R., et al. (2015). Measurements of methane emissions from natural gas gathering facilities and processing plants: Measurement methods. *Atmospheric Measurement Techniques, 8*(5), 2017-2035. https://doi.org/10.5194/amt-8-2017-2015

Saunois, M., Stavert, A. R., Poulter, B., Bousquet, P., Canadell, J. G., Jackson, R. B., et al. (2020). The global methane budget 2000–2017. *Earth System Science Data, 12*(3), 1561-1623. https://doi.org/10.5194/essd-12-1561-2020

Schwietzke, S., Sherwood, O. A., Bruhwiler, L. M., Miller, J. B., Etiope, G., Dlugokencky, E. J., et al. (2016). Upward revision of global fossil fuel methane emissions based on isotope database. *Nature, 538*(7623), 88-91. https://doi.org/10.1038/nature19797

Seinfeld, J. H., & Pandis, S. N. (2006). Chapter 18: Atmospheric Diffusion. In *Atmospheric Chemistry and physics: From air pollution to climate change* (2nd ed., pp. 851-886). Hoboken, NJ: Wiley.

Smith, M. L., Gvakharia, A., Kort, E. A., Sweeney, C., Conley, S. A., Faloona, I., et al. (2017). Airborne quantification of methane emissions over the Four Corners region. *Environmental Science & Technology, 51*(10), 5832-5837. https://doi.org/10.1021/acs.est.6b06107

Smith, M. L., Kort, E. A., Karion, A., Sweeney, C., Herndon, S. C., & Yacovitch, T. I. (2015). Airborne ethane observations in the Barnett Shale: Quantification of ethane flux and

attribution of methane emissions. *Environmental Science & Technology*, *49*(13), 8158-8166. https://doi.org/10.1021/acs.est.5b00219

SONGNEX 2015 [Dataset]. National Oceanic & Atmospheric Administration, Chemical Sciences Laboratory. Retrieved from: https://csl.noaa.gov/projects/songnex/

State of New Mexico, Secretary of Environment. Environmental Protection Division (2020). Settlement Agreement and Stipulated Final Compliance Order. AQB CCI-1252-1801-R2 (NOV). Retrieved from: https://www.env.nm.gov/wp-content/uploads/2020/11/2020-10-28-EPD-AQB-CCI-San-Juan-SASFCO-1252-1801-Final-for-signature.pdf

Toon, G. C. (2014). Atmospheric Line List for the 2014 TCCON Data Release. CaltechDATA. Retrieved from: https://doi.org/10.14291/TCCON.GGG2014.ATM.R0/1221656

TOPDOWN 2014 [Dataset]. National Oceanic & Atmospheric Administration, Chemical Sciences Laboratory. Retrieved from: https://csl.noaa.gov/groups/csl7/measurements/2014topdown/

Travis, B., Dubey, M., & Sauer, J. (2020). Neural networks to locate and quantify fugitive natural gas leaks for a MIR detection system. *Atmospheric Environment: X*, *8*, 100092. https://doi.org/10.1016/j.aeaoa.2020.100092

Tribby, A. L., Bois, J. S., Montzka, S. A., Atlas, E. L., Vimont, I., Lan, X., et al. (2022). Hydrocarbon tracers suggest methane emissions from fossil sources occur predominately before gas processing and that petroleum plays are a significant source. *Environmental Science & Technology*, *56*(13), 9623-9631. https://10.1021/acs.est.2c00927

Turner, A. J., Jacob, D. J., Wecht, K. J., Maasakkers, J. D., Lundgren, E., Andrews, A. E., et al. (2015). Estimating global and North American methane emissions with high spatial resolution using GOSAT satellite data. *Atmospheric Chemistry and Physics*, *15*(12), 7049-7069. https://doi.org/10.5194/acp-15-7049-2015

United States of America, Department of The Interior, Office of Surface Mining Reclamation and Enforcement. (2018). Draft Environmental Impact Statement for the San Juan Mine Deep Lease Extension. Retrieved from: https://www.wrcc.osmre.gov/initiatives/sanJuanMine/documents/052518_SanJuanMine_DraftEIS.pdf

United States of America, Environmental Protection Agency, Coalbed Methane Outreach Program. (2019). Identifying Opportunities for Methane Recovery at U.S. Coal Mines: Profiles of Selected Gassy Underground Coal Mines (2002-2016). Vol. EPA 430-K-18-001. Retrieved from: https://www.epa.gov/sites/default/files/2019-11/documents/epa_cmop_gassy_mine_profiles_2002-2016_final.pdf

Varon, D. J., Jacob, D. J., Jervis, D., & McKeever, J. (2020). Quantifying time-averaged methane emissions from individual coal mine vents with GHGSat-D satellite

observations. *Environmental Science & Technology*, *54*(16), 10246-10253. https://doi.org/10.1021/acs.est.0c01213

Viatte, C., Lauvaux, T., Hedelius, J. K., Parker, H., Chen, J., Jones, T., et. al. (2017). Methane emissions from dairies in the Los Angeles Basin. *Atmospheric Chemistry and Physics*, *17*(12), 7509-7528. https://doi.org/10.5194/acp-17-7509-2017

Vogel, F. R., Frey, M., Staufer, J., Hase, F., Broquet, G., Xueref-Remy, I., et al. (2019). XCO2 in an emission hot-spot region: The COCCON Paris campaign 2015. *Atmospheric Chemistry and Physics*, *19*(5), 3271-3285. https://doi.org/10.5194/acp-19-3271-2019

Wunch, D., Toon, G. C., Blavier, J. L., Washenfelder, R. A., Notholt, J., Connor, B. J., et al. (2011). The Total Carbon Column Observing Network. *Philosophical Transactions of the Royal Society A: Mathematical, Physical and Engineering Sciences*, *369*(1943), 2087-2112. https://doi.org/10.1098/rsta.2010.0240

Wunch, D., Toon, G. C., Hedelius, J. K., Vizenor, N., Roehl, C. M., Saad, K. M., et al. (2016). Quantifying the loss of processed natural gas within California's South Coast Air Basin using long-term measurements of ethane and methane. *Atmospheric Chemistry and Physics*, *16*(22), 14091-14105. https://doi.org/10.5194/acp-16-14091-2016

Wunch, D., Toon, G. C., Scherlock, V., Deutscher, N. M., Liu, C., Feist, D. G., & Wennberg, P. O. (2015). The Total Carbon Column Observing Network's GGG2014 Data Version. *California Institute of Technology, Carbon Dioxide Information Analysis Center, Oak Ridge National Laboratory, Oak Ridge, Tennessee, USA*. https://doi.org/10.14291/TCCON.GGG2014.DOCUMENTATION.R0/1221662

Yacovitch, T. I., Herndon, S. C., Roscioli, J. R., Floerchinger, C., McGovern, R. M., Agnese, M., et al. (2014). Demonstration of an ethane spectrometer for methane source identification. *Environmental Science & Technology*, *48*(14), 8028-8034. https://doi.org/10.1021/es501475q

Zhao, X., Marshall, J., Hachinger, S., Gerbig, C., Frey, M., Hase, F., & Chen, J. (2019). Analysis of total column CO2 and CH4 measurements in Berlin with WRF-GHG. *Atmospheric Chemistry and Physics*, *19*(17), 11279-11302. https://doi.org/10.5194/acp-19-11279-2019

References From the Supporting Information

Chen, J., Viatte, C., Hedelius, J. K., Jones, T., Franklin, J. E., Parker, H., et al. (2016). Differential column measurements using compact solar-tracking spectrometers. *Atmospheric Chemistry and Physics*, *16*(13), 8479-8498. https://doi.org/10.5194/acp-16-8479-2016

Heerah, S., Frausto- Vicencio, I., Jeong, S., Marklein, A. R., Ding, Y., Meyer, A. G., et al. (2021). Dairy methane emissions in California's San Joaquin Valley inferred with ground- based remote sensing observations in the summer and winter. *Journal of Geophysical Research: Atmospheres*, *126*(24). https://doi.org/10.1029/2021jd034785

Jones, T. S., Franklin, J. E., Chen, J., Dietrich, F., Hajny, K. D., Paetzold, J. C., et al. (2021). Assessing urban methane emissions using column-observing portable Fourier transform infrared (FTIR) spectrometers and a novel Bayesian inversion framework. *Atmospheric Chemistry and Physics, 21*(17), 13131-13147. https://doi.org/10.5194/acp-21-13131-2021

Seinfeld, J. H., & Pandis, S. N. (2006). Chapter 18: Atmospheric Diffusion. In *Atmospheric Chemistry and physics: From air pollution to climate change* (2nd ed., pp. 851-886). Hoboken, NJ: Wiley.

University of Utah, Department of Atmospheric Sciences (2022). MesoWest. Accessed May 5, 2022. Available at: https://mesowest.utah.edu/

Viatte, C., Lauvaux, T., Hedelius, J. K., Parker, H., Chen, J., Jones, T., et. al. (2017). Methane emissions from dairies in the Los Angeles Basin. *Atmospheric Chemistry and Physics, 17*(12), 7509-7528. https://doi.org/10.5194/acp-17-7509-2017

Vogel, F. R., Frey, M., Staufer, J., Hase, F., Broquet, G., Xueref-Remy, I., et al. (2019). XCO2 in an emission hot-spot region: The COCCON Paris campaign 2015. *Atmospheric Chemistry and Physics, 19*(5), 3271-3285. https://doi.org/10.5194/acp-19-3271-2019

Zhao, X., Marshall, J., Hachinger, S., Gerbig, C., Frey, M., Hase, F., & Chen, J. (2019). Analysis of total column CO2 and CH4 measurements in Berlin with WRF-GHG. *Atmospheric Chemistry and Physics, 19*(17), 11279-11302. https://doi.org/10.5194/acp-19-11279-2019